Neurosci. Bull. October, 2021, 37(10):1381–1396
https://doi.org/10.1007/s12264-021-00737-1

www.neurosci.cn
www.springer.com/12264

ORIGINAL ARTICLE

ASIC2 Synergizes with TRPV1 in the Mechano-Electrical Transduction of Arterial Baroreceptors

Xiaodong Yan[1] · Sitao Zhang[2] · Haiyan Zhao[3] · Ping Liu[1] · Haixia Huang[1] · Weizhen Niu[1] · Wei Wang[1,4] · Chen Zhang[5]

Received: 18 November 2020 / Accepted: 9 March 2021 / Published online: 2 July 2021

Abstract Mechanosensitive ion channels (MSCs) are key molecules in the mechano-electrical transduction of arterial baroreceptors. Among them, acid-sensing ion channel 2 (ASIC2) and transient receptor potential vanilloid subfamily member 1 (TRPV1) have been studied extensively and documented to play important roles. In this study, experiments using aortic arch–aortic nerve preparations isolated from rats revealed that both ASIC2 and TRPV1 are functionally necessary, as blocking either abrogated nearly all pressure-dependent neural discharge. However, whether ASIC2 and TRPV1 work in coordination remained unclear. So we carried out cell-attached patch-clamp recordings in HEK293T cells co-expressing ASIC2 and TRPV1 and found that inhibition of ASIC2 completely blocked stretch-activated currents while inhibition of TRPV1 only partially blocked these currents. Immunofluorescence staining of aortic arch–aortic adventitia from rats showed that ASIC2 and TRPV1 are co-localized in the aortic nerve endings, and co-immunoprecipitation assays confirmed that the two proteins form a compact complex in HEK293T cells and in baroreceptors. Moreover, protein modeling analysis, exogenous co-immunoprecipitation assays, and biotin pull-down assays indicated that ASIC2 and TRPV1 interact directly. In summary, our research suggests that ASIC2 and TRPV1 form a compact complex and function synergistically in the mechano-electrical transduction of arterial baroreceptors. The model of synergism between MSCs may have important biological significance beyond ASIC2 and TRPV1.

Keywords Acid-sensing ion channel 2 · Transient receptor potential vanilloid subfamily member 1 · Mechano-electrical transduction · Arterial baroreceptors · Synergism

Xiaodong Yan and Sitao Zhang have contributed equally to this work.

Supplementary Information The online version contains supplementary material available at https://doi.org/10.1007/s12264-021-00737-1.

✉ Wei Wang
wangwei@ccmu.edu.cn

✉ Chen Zhang
czhang@ccmu.edu.cn

[1] Department of Physiology and Pathophysiology, School of Basic Medical Sciences, Capital Medical University, Beijing 100069, China

[2] Department of Orthopedics, Xuanwu Hospital, Capital Medical University, Beijing 100053, China

[3] Yanjing Medical College, Capital Medical University, Beijing 101300, China

[4] Beijing Laboratory for Cardiovascular Precision Medicine, Capital Medical University, Beijing 100069, China

[5] Department of Neurobiology, School of Basic Medical Sciences, Beijing Key Laboratory of Neural Regeneration and Repair, Advanced Innovation Center for Human Brain Protection, Capital Medical University, Beijing 100069, China

Introduction

Blood pressure is a critical hemodynamic factor. The absence of proper regulation of blood pressure has important pathophysiological consequences. Maintaining the homeostasis of blood pressure is necessary to ensure that the body is prepared to meet its host of activities. The arterial baroreceptor reflex (also known as the depressor reflex) is a basic regulatory mechanism that maintains blood pressure within a relatively narrow physiological range, and it has been considered to be a potential target for

the treatment of cardiovascular diseases [1, 2]. Mechano-electrical transduction constitutes the first part of the depressor reflex and involves three steps: mechanical coupling, conversion of mechanical signals to receptor potentials, and the induction of action potentials. Baroreceptors are sensory nerve terminals located in the adventitia of the carotid sinus and aortic arch that serve as frontline sensors for changes in blood pressure and act as mechano-electrical transducers by converting mechanical forces from vessel walls into electrical signals in nerve fibers.

The conversion of mechanical signals into receptor potentials is mediated by mechanosensitive ion channels (MSCs). Several MSCs, such as acid-sensing ion channel 2 (ASIC2) [3], transient receptor potential vanilloid subfamily member 1 (TRPV1) [4], epithelial sodium channel (ENaC) [5], transient receptor potential cation channel subfamily C member 5 (TRPC5) [6], and PIEZOs [7], have been reported to be expressed in sensory nerve endings and to be involved in mechano-electrical transduction. However, when any one of these channels is absent or functionally impaired, the residual baroreflex is still observed, implying the involvement of other sensory molecules. The unique roles of these channels and the interactions between them have not been evaluated. Among these MSCs, TRPV1 and ASIC2 have been widely studied in recent years. TRPV1 contributes to the sensitivity of mouse bladder afferents to distension [8], selectively modulates gastric vagal afferent tension receptor mechanosensitivity [9], and acts as an acupuncture-responsive channel by sensing physical stimulation at the Zusanli acupoint (ST36) in mice [10]. Furthermore, functional TRPV1 channels are found in baroreceptive nerve endings where they act as mechanoreceptors for the detection of increased blood pressure and the maintenance of blood pressure homoeostasis [11]. However, some studies have suggested that TRPV1 is insensitive to membrane stretch in heterologous overexpression systems [12]. Whether TRPV1 is activated by mechanical stimuli directly or by other mechanically-sensitive molecules in mechano-electrical transduction remains unclear. ASIC2, the other MSC associated with baroreceptor activity, is a member of the degenerin/epithelial sodium/acid-sensitive ion channel (DEG/ENaC/ASIC) family [13]. ASIC2 is a non-voltage-gated channel [14] strongly expressed in the mammalian central and peripheral nervous systems [13, 15] as well as in ganglia and baroreceptor nerve terminals [3, 16]. Studies of ASIC2 transgenic and null mouse model have shown that baroreceptor signaling is decreased in ASIC2-null mice compared with that in ASIC2-overexpressing mice [3]. Although these studies suggest key roles for ASIC2 and TRPV1 as mediators of mechano-electrical transduction in baroreceptors, i.e., both are indispensable. However, whether there is a correlation between these two MSCs and if they influence each other is currently unknown.

In the current study, we investigated the roles of ASIC2 and TRPV1 in the mechano-electrical transduction of baroreceptors. We used electrophysiological experiments, immunoelectron microscopy, co-immunoprecipitation (co-IP), molecular dynamics modeling, and biotin pull-down assays to determine if ASIC2 and TRPV1 interact with each other physically and functionally. Our study of ASIC2 and TRPV1 sheds light on the cooperation of MSCs in mechano-electrical transduction.

Materials and Methods

Animals

Experiments were conducted using specific-pathogen-free male Sprague-Dawley rats (Charles River) aged between 7 and 8 weeks (220 ± 10 g). The rats were individually housed and were cared for in strict accordance with the Guiding Principles for the Care and Use Committee of Capital Medical University. All animal experimental procedures were approved by the Institutional Animal Care and Use Committee of Capital Medical University, Beijing, China, and were performed in accordance with the "Regulations for the Administration of Affairs Concerning Experimental Animals" (by the State Science and Technology Commission, China, 1988). Ethics approval was obtained from the Animal Ethics Committee of Capital Medical University.

Electrophysiological Experiments

The rats were anesthetized with an intraperitoneal injection (5 mL/kg) of urethane (2 g/L) and were mechanically ventilated with air.

Aortic Arch-Aortic Nerve Preparation

A midline incision was made in the neck and upper chest. The sternum was cut with operating scissors, and the upper chest was opened. The trachea was cannulated and ventilated (Animal Ventilator, HX-300S, Chengdu Techman Software Co. Ltd). The ascending aorta, descending aorta, pulmonary trunk, left common carotid artery, left subclavian artery, and aortic nerve were exposed and separated under a stereomicroscope (SMZ 745T, Nikon, Japan).

Recording of Pressure-Dependent Discharges

Each aortic arch–aortic nerve preparation was placed in a dish with perfusion fluid gassed with 100% O_2. The pulmonary trunk, left common carotid artery, and left subclavian artery were ligated, and the ascending aorta and descending aorta were cannulated as the inlet and outlet for perfusion, respectively. At the same time, the aortic nerve was placed on the recording electrode. Vascular pressure was procedurally controlled (80 mmHg–120 mmHg pulsatile pressure) with a custom-made pressure-servo system containing an auto-regulating valve (PRE-U, Hoerbiger, Germany) as a key element (Fig. S1); at the same time, the nerve discharges were recorded. A computer-operated pressure-control valve (PRE-U), which controlled high-pressure pure O_2 (0.5 MPa) and output a predetermined pressure, was used to push the perfusate in the liquid storage bottle into the blood vessel. The perfusate contained the following (mmol/L): 140 NaCl, 6 KCl, 1.1 $CaCl_2$, 1.2 $MgSO_4$, 5.5 glucose, and 10 HEPES. The pH was adjusted with HEPES-NaOH to 7.38–7.42 at 37°C. The perfusate was aerated with 100% O_2 to inhibit the chemoreceptors. The afferent activity of the nerve was amplified by a factor of 5000, filtered with a passband of 300 Hz to 10 kHz, and digitized at 20 kHz with a data acquisition system (Cyber Amp 380, pCLAMP 10.0 and Digidata 1440, Axon Instruments, USA).

Analysis of Baroreceptor Discharges

The baroreceptor discharges were analyzed offline with Spike2 (Cambridge Electronic Design Ltd, UK). The sharp power spectrum peaked at 50 Hz, and its multiples in the raw recordings were subtracted digitally with band-stop filters. In our recordings, the spikes were normally biphasic waves, consisting of an initial large, brief, and rapidly-evolving negative phase (approximately 0.5 ms) followed by a smaller, longer, and slower positive phase (0.5–1.5 ms).

Immunofluorescence Staining

After harvesting the aortic arch–aortic nerve preparations, the vascular endothelium was peeled away while retaining the vascular adventitia and aortic nerve. The tissues were fixed in 4% paraformaldehyde at 4°C overnight, then placed in 1 mL of 1% TBS-TWEEN for 5 min and incubated with 3% BSA at 4°C overnight. The tissues were then incubated with a primary antibody mixture containing guinea-pig anti-TRPV1 (Neuromics, 1:100), goat anti-ASIC2 (Santa Cruz, 1:100), and mouse anti-NF-L (neurofilament light polypeptide) antibodies (Santa Cruz, 1:200) at 4°C overnight. Next, the tissues were placed in 1 mL of 0.3% TBS-TWEEN for 5 min, and incubated for 2 h at room temperature with secondary antibodies (Jackson ImmunoResearch, 1:200) conjugated to Cytm2, Alexa Fluor 594, and Alexa Fluor 405. The distribution of aortic nerve terminals on the stained tissue was observed under a laser scanning confocal microscope (TCS-SP5, Leica).

Single-Channel Patch-Clamp Recordings

Patch-clamp experiments were carried out at room temperature. The cells with successful expression and distinguished by fluorescence were used for subsequent experiments. The pipettes were made of borosilicate glass (BF150–110–10; Sutter Instruments, Novato, CA) and had a resistance of 4–6 MΩ. The solutions used for the single-channel recording of TRPV1 and ASIC2 currents have been described previously [17, 18]. For TRPV1, the pipette solution contained (in mmol/L) 10 NaCl, 140 CsCl, 1 $MgCl_2$, 5 ethyleneglycoltetraacetic acid (EGTA), 2 MgATP, 0.03 Na_2GTP and 10 HEPES, pH adjusted to 7.4; the bath solution contained (in mmol/L) 140 NaCl, 4 CsCl, 1 $MgCl_2$, 1 EGTA, 10 HEPES, and 10 glucose, pH adjusted to 7.4. For ASIC2, the pipette solution contained (in mmol/L) 120 sodium gluconate, 30 NaCl, and 1 $CaCl_2$, pH adjusted to 7.4; the bath solution contained (in mmol/L) 150 NaCl and 1 $CaCl_2$, pH adjusted to 7.4. For cells co-expressing ASIC2 and TRPV1, the solutions for single-channel patch-clamp were the same as those for TRPV1. The HEKA EPC-10 patch-clamp amplifier and associated software (PULSE and PatchMaster; HEKA Electronic) were used to amplify the channel currents. Negative pressure was delivered to the patches using a pressure-generating device (DALE20 Pneumatic Transducer Tester; Luke Biomedical, Liverpool, UK). Data were analyzed using Clampfit software (Axon Instruments, Union City, CA) to obtain the channel current amplitude and the open probability. NP_O was used to represent the channel currents, where N is the number of channels and P_O is the open probability of a single channel. The analysis was as we previously reported [19].

Immunoelectron Microscopy

The vascular adventitia of each 4% formaldehyde-fixed rat aorta was cut into small pieces, postfixed in 2% glutaraldehyde for 2 h, washed twice for 10 min each with 0.1 mol/L PBS, placed in cane sugar for 2 h, and washed twice for 10 min each with 0.1 mol/L PBS. The pieces were then incubated with a primary antibody mixture containing guinea-pig anti-TRPV1 antibodies (Neuromics, 1:100) and goat anti-ASIC2 antibodies (Santa Cruz, 1:100) for 12 h at 4°C; washed twice with 0.1 mol/L PBS for 10 min each; incubated with 18 nm Colloidal Gold AffiniPure Donkey

Anti-Guinea-Pig IgG (H+L) (Jackson ImmunoResearch, 1:100), and 4 nm Colloidal Gold AffiniPure Donkey Anti-Goat IgG (H+L) (Jackson ImmunoResearch, 1:150) diluted in 0.1 mol/L borate-buffered saline (BBS) for 18 h at 4°C; washed twice with 0.1 mol/L BBS for 10 min each; washed with 0.1 mol/L PBS for 10 min; incubated with 1% osmic acid for 1.5 h; and washed three times with 0.1 mol/L PBS for 10 min each. Next, the tissues were soaked in 50% ethanol for 15 min, 70% ethanol for 15 min, 85% ethanol for 15 min, 90% ethanol for 15 min, 100% ethanol for 30 min, an ethanol:acetone (1:1) mixture for 10 min, and 100% acetone for 15 min; finally, the tissues were fixed in acetone:Epon 812 resin. Then, sections of the embedded tissues (70 nm) were cut Digital micrographs were processed with Adobe Photoshop CS5 (64-bit). An image acquisition and analysis system (Leica, Germany) was used to analyze the distribution of colloidal gold particles.

Plasmid Construction

The ASIC2 (NM_001034013.2) channel cDNA was fused at the 3′ end with the gene encoding the enhanced green fluorescent protein (EGFP) and an myc tag, and cloned into the pcDNA3.1 vector (Plasmid constructs were from KeyGEN BioTECH, Jiangsu, China). The resulting vector was transiently transfected into HEK293T cells, and GFP expression was used as a marker of successful transfection. The TRPV1 (NM_001001445.2) channel cDNA was fused at the 3′ end with the gene encoding mCherry and a hemagglutinin (HA) tag and cloned into the pcDNA3.1 vector. The resulting vector was transiently transfected into HEK293T cells, and mCherry expression was used as a marker of successful transfection. We also constructed the ASIC2 (59–427)-3×Flag plasmid, TRPV1 (455–472)-myc-GFP plasmid, TRPV1 (499–511)-myc-GFP plasmid, and TRPV1 (533–536)-myc-GFP plasmid for the subsequent exogenous co-IP experiments.

Cell Culture and Transfection

Human embryonic kidney 293T (HEK293T) cells were obtained from the Kunming Cell Bank, Chinese Academy of Sciences (Kunming, China) and cultured with Dulbecco's modified Eagle's medium (DMEM, Hyclone) and 10% fetal bovine serum (FBS, Gibco). ASIC2 and TRPV1 plasmids were transfected into HEK293T cells using Lipofectamine 3000 (Invitrogen, Carlsbad, CA). The HEK293T cells were cultured in a 6-well culture dish and transfected with ASIC2 or TRPV1 DNA (1.5 μg/well) or co-transfected with ASIC2 and TRPV1 DNA (0.75 μg/well). Fluorescence was observed to determine the transfection efficiency after 24 h of transfection, and the successfully transfected cells were used in subsequent experiments.

Co-immunoprecipitation and Western Blotting

ASIC2/TRPV1 co-transfected HEK293T cells, baroreceptor tissues from the aortic arches of adult Sprague-Dawley rats, or HEK293T cells expressing ASIC2(59–427)-3×Flag + TRPV1 (455–472)-myc-GFP, ASIC2(59–427)-3×Flag + TRPV1 (499–511)-myc-GFP, or ASIC2(59–427)-3×Flag + TRPV1(533–536)-myc-GFP were lysed in IP lysis buffer (C1054; Applygen Technologies Inc.) with Phenylmethanesulfonyl fluoride (PMSF) (ST506; Beyotime Biotechnology, Shanghai, China) and protease inhibitor cocktail (Roche) for 30 min in an ice bath. A total of 100 μL of the sample was used for input, and the rest of the sample was used for co-IP. Each sample was centrifuged at 14,000 rpm at 4°C for 15 min to remove the insoluble materials. The supernatants were collected and pre-cleared with Protein A/G immunoprecipitation beads.

The supernatants were combined with 1 μg anti-ASIC2 or anti-TRPV1 antibodies/mg protein for the extraction of protein from aortic arch baroreceptor tissues. The dilution ratios of anti-Flag, anti-myc, and anti-HA antibodies for the extraction of protein from transfected HEK293T cells are listed in the key resources table. These mixtures were incubated at 4°C for 8–12 h with gentle rotation on a rotary table, followed by extensive washing. For western blotting, supernatants were boiled in 5×SDS loading buffer. Protein samples were separated *via* sodium dodecyl sulfate-polyacrylamide gel electrophoresis (8–12% SDS-PAGE depending on the molecular weight of the protein of interest) with SDS-PAGE Running Buffer (Applygen Technology, B1005). Proteins were transferred to polyvinylidene fluoride (PVDF) membranes (Millipore, Billerica, MA, USA) and incubated with primary anti-ASIC2 (1:1000), anti-TRPV1 (1:1000), or anti-myc (1:1000), anti-HA (1:1000), and anti-Flag (1:1000) antibodies at 4°C overnight, then incubated with horseradish peroxidase-conjugated rabbit or mouse secondary antibodies for 1 h at room temperature. Immunoreactivity was visualized with an electrochemiluminescence detection system. Immunoprecipitation with normal rabbit or mouse serum was used to produce negative controls.

Molecular Dynamics Modeling and Protein Analysis

The three-dimensional structures of the mouse ASIC2 (NP_001029185.1) and TRPV1 (NP_001001445.1) were obtained using the homology modeling method with a single template (3IJ4: 62.53%, 5IRZ: 98.10%) with Modeller software [20]. Protein-protein docking was implemented to explore possible binding interfaces

between mouse ASIC2 and TRPV1. Docking simulations were performed with Rosetta software, and a total of 100 conformations were extracted and ranked by docking energy value. Finally, the best docking conformation with the lowest docking score was selected for further molecular dynamics (MD) simulation analysis. The initial position of the protein was found manually and refined using Rosetta. MD studies of the protein-protein complexes were performed using GROMACS software and the AMBER99SB force field. ASIC2 and TRPV1 complexes were inserted into a 1-palmitoyl-2-oleoyl-sn-glycero-3-phosphocholine membrane and hydrated, and ions were added to neutralize protein charges and then to reach a concentration of 0.15 mol/L NaCl. The size of each simulation box was approximately 85 Å × 92 Å × 128 Å. The complexes were minimized and subjected to an MD stimulus, first in the NVT ensemble (constant number of particles, volume, and temperature) for 1 ns, then continued 20 ns in the NPT ensemble (constant number of particles, pressure, and temperature); in each case, the protein backbone was restricted. The production run was performed in the NPT ensemble with no restrictions for 100 ns. Analysis of the MD simulations was performed with GROMACS.

Biotin Pull-Down Assays

The purified recombinant mouse GST-tagged ASIC2 extracellular segment [amino-acids (aa) 59–427] (KeyGEN BioTECH) and biotin-labeled mouse TRPV1 peptides (aa 455–472, aa 499–511, and aa 533–536) (GeneCreate Biological Engineering Co., Ltd., Wuhan, China) were each mixed and incubated on ice for 3 h. Solid-phase synthesis, reversed-phase high-performance liquid chromatography purification, and matrix-assisted laser dissociation time-of-flight mass spectrometry were used to identify a series of peptides containing "biotin-aa 455–472" sequences, "biotin-aa 499–511" sequences, and "biotin-aa 533–536" sequences. The TRPV1 intracellular segment, aa 499–511, was used as a negative control. Subsequently, each mixture was incubated with Streptavidin magnetic beads (New England Biolabs, USA). After washing five times with wash buffer, proteins were eluted with wash buffer supplemented with 15 mM reduced glutathione. The eluates were separated on 12% SDS-PAGE, transferred to PVDF membranes (Millipore, Billerica, MA, USA), and probed with anti-GST antibodies (Sigma-Aldrich, Merck KGaA, Darmstadt, Germany). GST from Wuhan Genecreate (Wuhan, China) was used as the negative control.

Statistical Analysis

All data were analyzed using Prism 5.01 (GraphPad Software, La Jolla, CA). Data are expressed as the mean ± standard error. One-way repeated-measures analysis of variance (ANOVA) was used to analyze pressure-dependent discharges of the aortic arch–aortic nerve and the mechanosensitivity under different negative pressures. Paired *t*-tests were used to compare data obtained before and after a negative pressure intervention and data obtained from different groups at a specific pressure. P values <0.05 were considered to be significant.

Results

Inhibition of ASIC2 Blocks Almost All Pressure-Dependent Discharges in Aortic Baroreceptors

In order to evaluate the function of ASIC2 and TRPV1 in baroreceptors, we used aortic arch–aortic nerve preparations from rats, and recorded pressure-dependent discharges before and after perfusion with the ASIC2 antagonists amiloride or benzamil using a custom-made pressure-servo system (Fig. S1). The drug concentrations used were based on previous reports [21, 22]. Perfusion of amiloride (100 μmol/L), an ASIC2-selective antagonist, decreased the pressure-dependent discharges from 97.07 ± 1.80 spikes/cycle to 17.47 ± 0.79 spikes/cycle (Fig. 1A, B). Benzamil (16–128 μmol/L), a more specific ASIC2 antagonist, was used to confirm the function of ASIC2. The results showed that benzamil inhibited the pressure-dependent discharges in a concentration-dependent manner (Fig. 1C). Benzamil at low concentrations (16 μmol/L and 32 μmol/L) exhibited a mild inhibitory effect on aortic nerve discharges after 15 min (from 98.97 ± 0.65 to 74.1 ± 1.49 spikes/cycle, and from 98.97 ± 0.65 to 26.63 ± 1.00 spikes/cycle, while at high concentration (128 μmol/L) it suppressed most of the discharges in only 2–3 min (98.97 ± 0.65 to 5.05 ± 0.33 spikes/cycle) (Fig. 1D, E). When benzamil was removed by washing, the frequency of discharges recovered, indicating that the blocking effect is reversible (Fig. 1C, D).

Inhibition of TRPV1 Blocks Nearly All Pressure-Dependent Discharges in Aortic Baroreceptors

Perfusion with RR (20 μmol/L), a TRP-selective antagonist, decreased the pressure-dependent discharges from 98.31 ± 0.60 to 22.53 ± 1.69 spikes/cycle (Fig. 2A, B). Capsazepine (10 μmol/L–50 μmol/L), a TRPV1-selective antagonist, was used to confirm the function of TRPV1. The drug concentrations used were based on previous

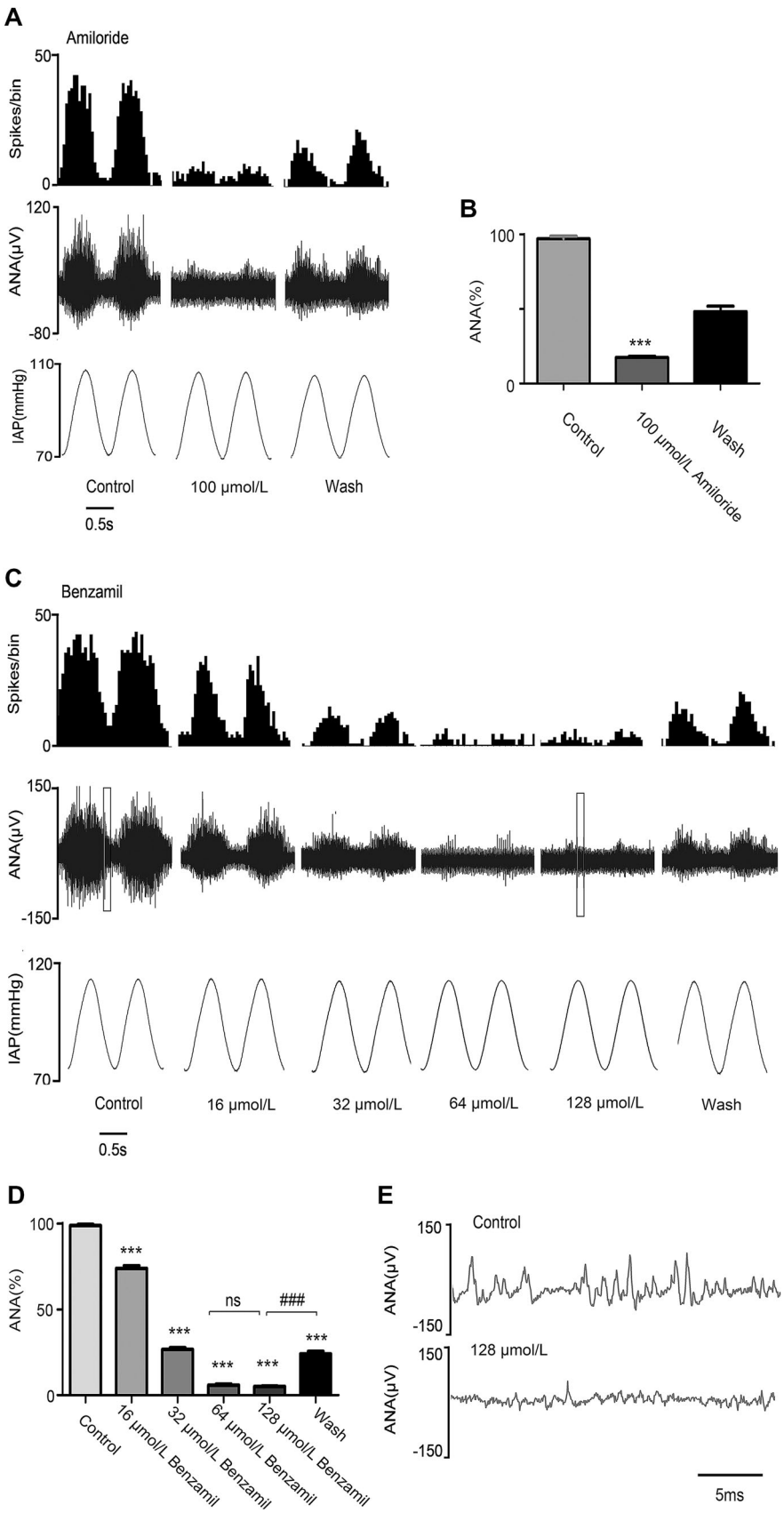

Fig. 1 Effects of blocking ASIC2 on aortic arch baroreceptor discharges. **A** Baroreceptor discharges recorded in rat aortic arch nerve preparations under pulsatile pressure before (control group) and after perfusion of 100 μmol/L amiloride, and after removal of the amiloride by washing with perfusate (wash group). **B** Statistical analysis of the effect of 100 μmol/L amiloride (n = 5; $^{***}P$ <0.001 *vs* control group). **C** Baroreceptor discharges recorded before (control group) and after perfusion with different concentrations of benzamil, and after removal of benzamil by washing with perfusate (wash group). **D** Statistical analysis of the effect of benzamil (n = 3; $^{***}P$ <0.001 *vs* control group, $^{\#\#\#}P$ <0.001 *vs* wash group; binwidth, 0.05 s). **E** Expansion of the boxed area in (**C**). ANA, aortic nerve activity; IAP, intravascular aortic pressure. 1 mmHg = 0.133 kPa.

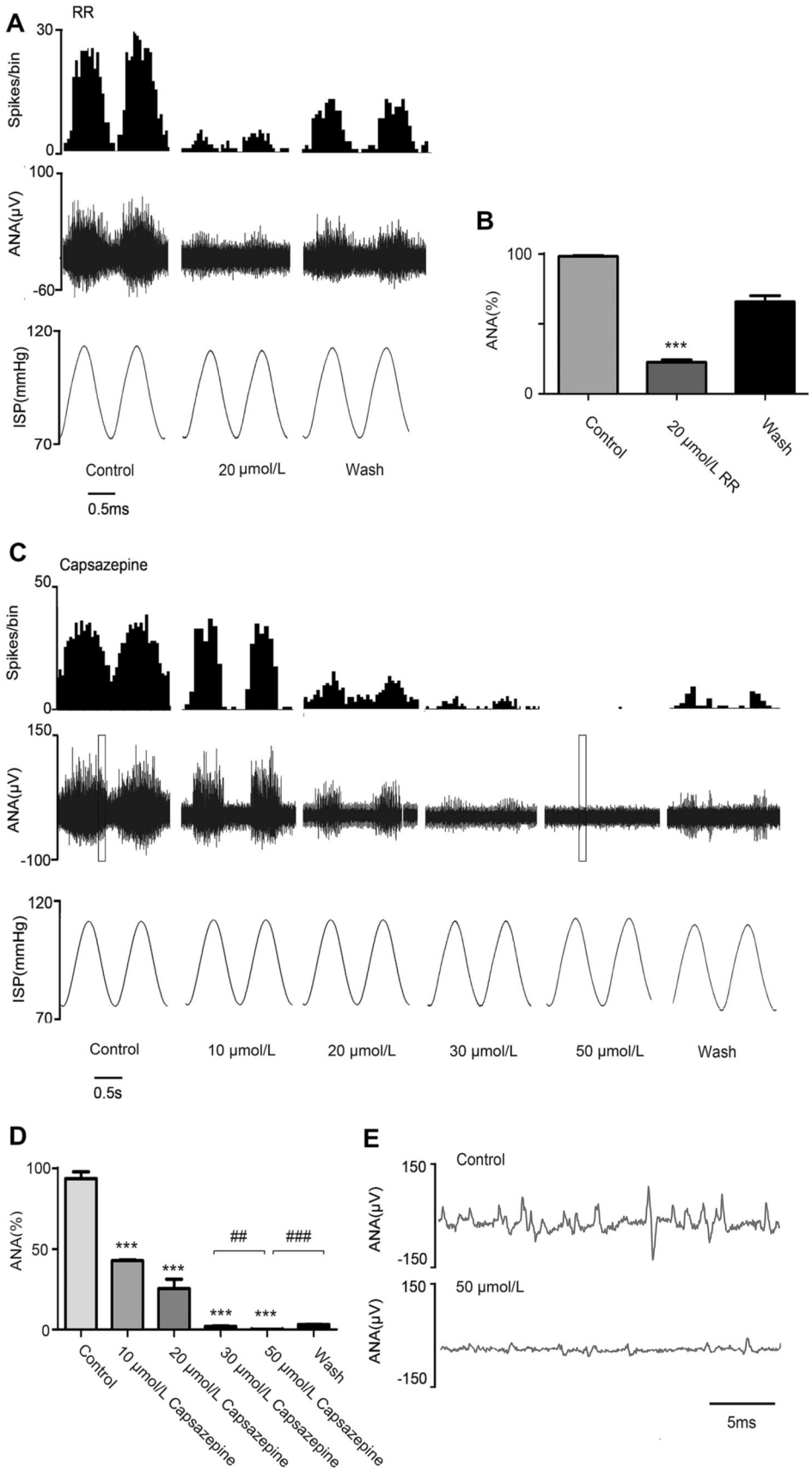

Fig. 2 Effects of blocking TRPV1 on aortic arch baroreceptor discharges. **A** Baroreceptor discharges recorded before (control group) and after perfusion with 20 μmol/L ruthenium red (RR), and after removal of RR with perfusate (wash group). **B** Statistical analysis of the effect of 20 μmol/L RR ($n = 4$; $^{***}P < 0.001$ *vs* control group). **C** Baroreceptor discharges recorded before (control group) and after perfusion with different concentrations of capsazepine, and after removal of capsazepine with perfusate (wash group). **D** Statistical analysis of the effect of capsazepine ($n = 3$; $^{***}P < 0.001$ *vs* control group, $^{\#\#}P < 0.01$ for 30 μmol/L *vs* 50 μmol/L capsazepine, $^{\#\#\#}P < 0.001$ for wash *vs* 50 μmol/L capsazepine; binwidth, 0.05 s). **E** Expansion diagram of the boxed area in (**C**). ANA, aortic nerve activity. IAP, intravascular aortic pressure. 1 mmHg = 0.133 kPa.

reports [23, 24]. The results showed that capsazepine inhibited the pressure-dependent discharges in a concentration-dependent manner (Fig. 2C). Capsazepine at low concentrations (10 μmol/L and 20 μmol/L) had a mild inhibitory effect on aortic nerve discharges after 7 min (10 μmol/L: 93.74 ± 4.19 to 42.85 ± 0.42 spikes/cycle, 20 μmol/L: 93.74 ± 4.19 25.46 ± 5.83 spikes/cycle), while interestingly, we found that capsazepine inhibited pressure-dependent discharges completely at high concentration (50 μmol/L) in 5–7 min (93.74 ± 4.19 to 0.14 ± 0.08 spikes/cycle) (Fig. 2D, E) and this effect was also reversible. When either ASIC2 or TRPV1 was blocked, the pressure-dependent discharge was almost completely abolished, and there was no compensatory effect of the other channel. Therefore, their functions in mechano-electrical transduction and their contributions to aortic pressure-dependent discharges are co-dependent.

The Mechanosensitivity of ASIC2 is Greater than that of TRPV1

The above functional experiments showed that both ASIC2 and TRPV1 are required for the discharge of aortic arch baroreceptors. To explore the role of these MSCs further, we expressed ASIC2 and/or TRPV1 in HEK293T cells, and carried out patch-clamp experiments to assess the mechanosensitivity of the two channels. Single-channel currents were recorded continuously in cell-attached mode at −100 mV, and the effects of membrane stretching (negative pressures from −10 mmHg to −30 mmHg) on the activity of ASIC2 and TRPV1 were analyzed.

First, ASIC2 and TRPV1 were effectively expressed, either individually or together, in HEK293T cells (Fig. S2A). The activity of ASIC2 markedly increased with negative pressure and returned to basal levels when the negative pressure was removed (n = 6 cells, Fig. 3A, C), while the activity of TRPV1 was much weaker compared with ASIC2 (n = 7 cells, Fig. 3B, C).

The relationship between the total single-channel open probability (NP_O) and negative pressure was fitted by NP_O=Ae^{kx}, where A is the background activity, x is the pressure, and k is the slope, reflecting the mechanosensitivity in units of 1/mmHg. The NP_O values of ASIC2 and TRPV1 channels are listed in Table 1. The fitted equations were $NP_O = 0.003e^{0.1329x}$ (R^2 = 0.8468, n = 6 cells) for ASIC2 and $NP_O = 0.001e^{0.0774x}$ (R^2 = 0.8121, n = 7 cells) for TRPV1, which more intuitively show that the mechanosensitivity of TRPV1 is much smaller than that of ASIC2 (Fig. 3D).

We performed the same experimental procedure in HEK293T cells co-expressing ASIC2 and TRPV1 (n = 9 cells. Fig. 3E). The all-point histogram analysis of channel opening events in cells expressing ASIC2 alone (Fig. 3Fa) as well as cells co-expressing ASIC2 and TRPV1 (Fig. 3Fb) showed that there were two conductance states in the ASIC2-TRPV1 co-expressing cells, while only one conductance state occurred in the cells expressing ASIC2 alone, indicating that two distinct channels were activated by cell membrane stretching in the ASIC2-TRPV1 co-

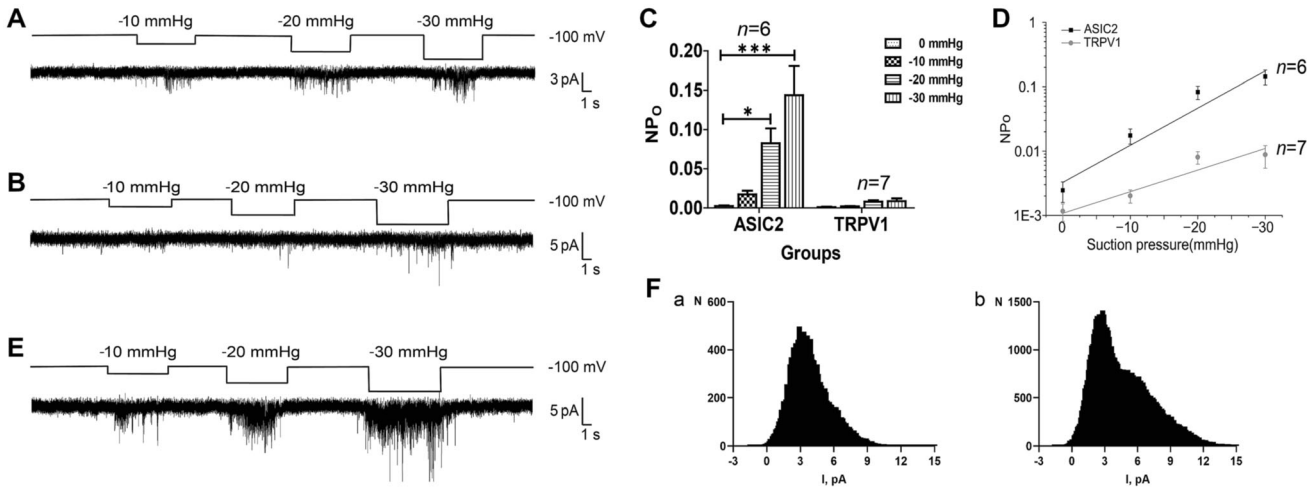

Fig. 3 Mechanosensitivity of ASIC2 and TRPV1. **A** Effects of membrane stretching on the activity of ASIC2 in HEK293T cells expressing ASIC2 alone. **B** Effects of membrane stretching on the activity of TRPV1 in HEK293T cells expressing TRPV1 alone. **C** Quantification of the pressure effect on *NPo* of ASIC2 or TRPV1 channels expressed in HEK293T cells. For each channel, *NPo* was calculated from 0 to − 30 mmHg pressure. **D** Pressure-dependence of ASIC2 activity (black) and TRPV1 activity (grey). **E** Effects of membrane stretching on the activity of channels in HEK293T cells co-expressing ASIC2 and TRPV1. **F** All-point histogram analysis of channel opening events for a cell expressing ASIC2 alone (a) and a cell co-expressing ASIC2-TRPV1 (b) (*P <0.05, ***P <0.001 *vs* 0 mmHg, ANOVA with *post hoc* analysis), NP_O, total single-channel open probability.

Table 1 NP_O of ASIC2 and TRPV1 currents at different negative pressures.

	0 mmHg	–10 mmHg	–20 mmHg	–30 mmHg	*n*
ASIC2	0.0025 ± 0.0009	0.0174 ± 0.0046	0.0827 ± 0.0190*	0.1439± 0.0370***	6
TRPV1	0.0012 ± 0.0004	0.0020 ± 0.0005	0.0080 ± 0.0018*	0.0088 ± 0.0034*	7

Values are means ± standard error; *n*, number of cell-attached patches. *P <0.05, ***P <0.001 *vs* 0 mmHg (ANOVA with *post hoc* analysis)

expressing cells. The stretch-activated current activity was markedly increased in cells co-expressing ASIC2 and TRPV1 compared to those expressing ASIC2 or TRPV1 alone under various negative pressure conditions (Fig. 3E). These results suggest that ASIC2 is activated by cell membrane stretching as a mechanosensor, while TRPV1 is more likely to be activated subsequent to ASIC2 activation and acts as an amplifier of the cellular mechanosensory signaling cascades.

ASIC2 Inhibition, but not TRPV1 Inhibition, Nearly Abolishes Stretch-Activated Currents in Cells Overexpressing ASIC2 and TRPV1

We co-transfected HEK293T cells with vectors for the expression of ASIC2 and TRPV1 and measured single-channel currents stimulated by negative pressure using the patch-clamp method before and after treatment with benzamil or capsazepine. Based on the above findings, we selected −30 mmHg as the negative pressure for subsequent experiments.

First, to confirm the absence of any cross-reactive interference due to the drugs used in this study, HEK293T cells transfected with ASIC2 or TRPV1 alone were treated with either 100 μmol/L benzamil or 20 μmol/L capsazepine (Fig. S2B–H). Single-channel currents were recorded continuously in cell-attached mode (Fig. S2B), and the drug concentrations used were based on previous reports [22, 25–28]. As expected, benzamil effectively inhibited the stretch-activated activity of ASIC2 (Fig. S2C) without affecting the activity of TRPV1 (Fig. S2G), while capsazepine blocked the weak activation of TRPV1 under negative pressure stimulation (Fig. S2H) without affecting the stretch-activated activity of ASIC2 (Fig. S2D). These results confirmed that there was no cross-reactivity in the inhibitory functions of the drugs.

Second, ASIC2 and TRPV1 were co-expressed effectively in HEK293T cells (Fig. S2A). The current activity was recorded under −30 mmHg in the DMSO control group (n = 16 cells; Fig. 4A). Treatment with 100 μmol/L benzamil completely abolished the current activity in response to negative pressure (n = 6 cells; Fig. 4B, D). By contrast, the stretch-activated currents were only slightly reduced after treatment with 20 μmol/L capsazepine (n = 8 cells; Fig. 4C, D). In addition, the all-point histogram analysis of channel-opening events in a cell co-expressing ASIC2 andTRPV1 (DMSO control group) indicated the presence of two distinct conductance states (Fig. 4Ea); therefore, two channels were activated in the ASIC2-TRPV1 co-expressing cell. After treatment with 20 μmol/L capsazepine, the all-point histogram analysis of channel-opening events showed only one conductance state (Fig. 4Eb) consistent with the conductance of ASIC2.

Taken together, the above results show that the stretch-activated currents were markedly increased in cells co-expressing ASIC2 and TRPV1 compared with those expressing either ASIC2 or TRPV1 alone (Fig. 3E), and no stretch-activated currents were detected in the co-expression system when ASIC2 activity was specifically blocked by benzamil (Fig. 4B, D), while a reduced frequency of currents was still activated in the co-expression system after treatment with the TRPV1-specific antagonist capsazepine (Fig. 4C, D). Thus, the stretch sensitivity of TRPV1 was affected by ASIC2 when they were co-expressed. If either channel was blocked, the pressure-dependent discharge was almost completely abolished (Figs. 1, 2). It is reasonable to hypothesize that the mechanical activation of ASIC2 alone is not sufficient for mechano-electrical transduction to induce action potentials or baroreceptor nerve discharge. Mechanic activation of TRPV1 may require ASIC2 when they are expressed together and may function as an amplifier in the cellular mechano-electrical transduction process. These results demonstrate that ASIC2 and TRPV1 contribute to the mechano-electrical transduction of baroreceptors in an synergistic manner.

ASIC2 Interacts with TRPV1 by Forming a Compact Complex in Baroreceptors

The *in vitro* results described above suggest that ASIC2 and TRPV1 have an synergistic effect on the mechano-electrical transduction of baroreceptors. However, it is still not clear how they achieve this function. To disclose the natural location of these two channels, we prepared aortic vascular adventitia (baroreceptors) specimens from rats to investigate the expression and organizational distribution of ASIC2 and TRPV1. Both ASIC2- and TRPV1-specific immunofluorescence signals were detected in the aortic vascular adventitia and merged well with signals of the

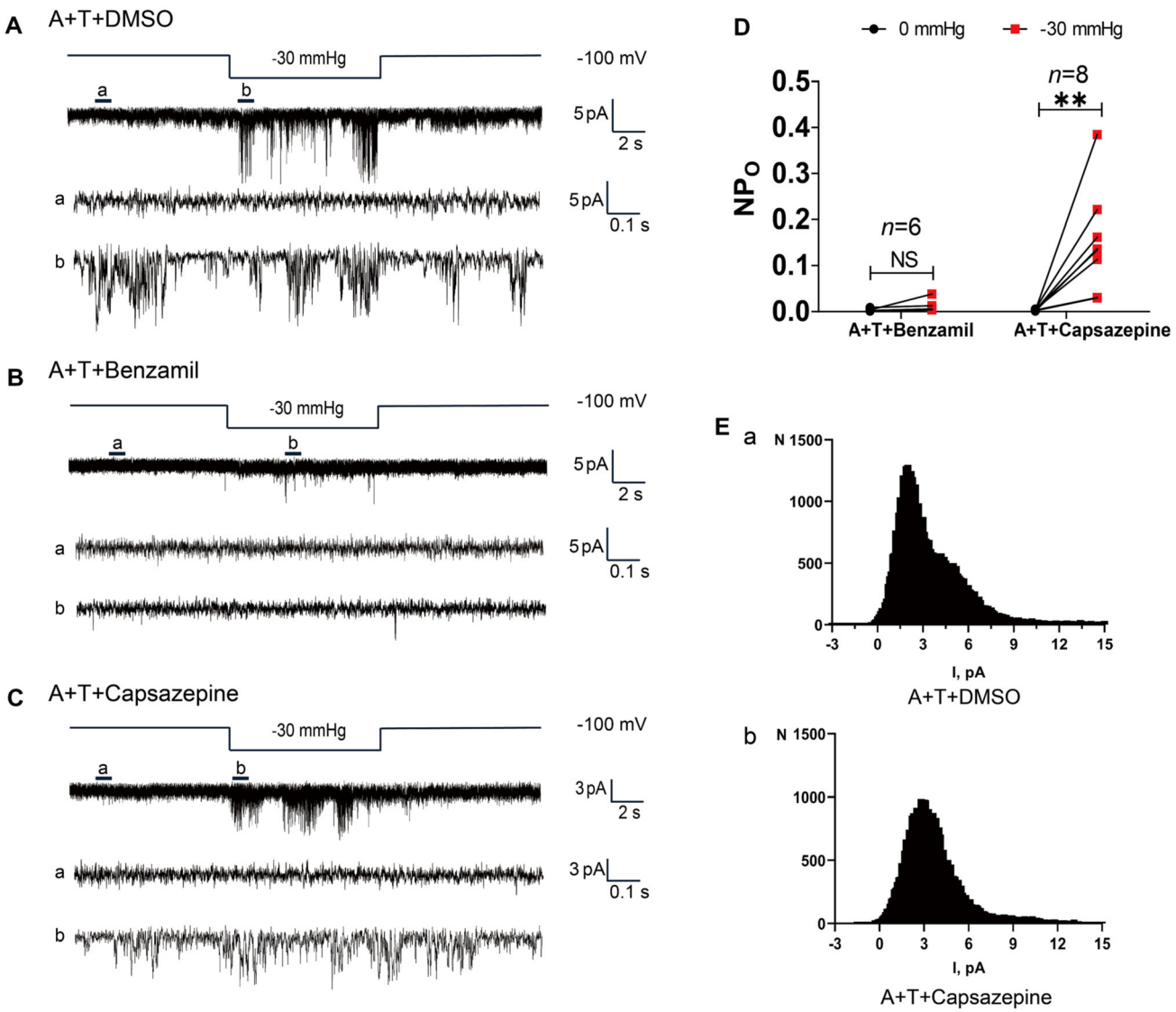

Fig. 4 Effects of blocking ASIC2 or TRPV1 on stretch-activated currents in cells overexpressing ASIC2 and TRPV1. **A** Upper traces, effects of negative pressure on currents from HEK293T cells co-expressing ASIC2 and TRPV1 (DMSO control group). Lower traces, expanded 1-s segments from 0 (**a**) and −30 mmHg (**b**). **B** Upper traces, channel activation in HEK293T cells co-expressing ASIC2 and TRPV1 after treatment with 100 μmol/L benzamil. Lower traces, expanded 1-s segments from 0 (**a**) and −30 mmHg (**b**). **C** Upper panels, effects of negative pressure on currents from HEK293T cells co-expressing ASIC2 and TRPV1 treated with 20 μmol/L capsazepine. Lower traces, expanded 1-s segments from 0 (**a**) and −30 (**b**) mmHg. **D** Quantification of the pressure effect on *NPo* of channels expressed in HEK293T cells before and after treatment with 100 μmol/L benzamil or 20 μmol/L capsazepine. **E** All-point histogram analysis of channel opening events for a cell co-expressing ASIC2-TRPV1 from (**a**) the DMSO control group, and (**b**) after treatment with 20 μmol/L capsazepine (**P <0.01, NS not significant *vs* 0 mmHg, paired *t*-test). NP_O, total single-channel open probability; A + T, co-expression of ASIC2 and TRPV1.

neurofilament marker NF-L (Fig. 5A). TRPV1 co-localized with ASIC2 in the baroreceptors, and ASIC2 and TRPV1 co-localized in the same baroreceptor nerve fiber (n = 6; Fig. 5A). Furthermore, we used immunoelectron microscopy to locate ASIC2 and TRPV1 in the tissue microstructure. ASIC2 was located close to TRPV1 at a distance of approximately 30 nm (n = 3; Fig. 5B). Therefore, the naturally-located mode of the two channels suggests the possibility that ASIC2 and TRPV1 form a protein complex.

To investigate whether the ASIC2 and TRPV1 channels physically interact, we first overexpressed myc-tagged ASIC2 and HA-tagged TRPV1 in HEK293T cells, then performed exogenous co-immunoprecipitation, which confirmed the interaction of recombinant ASIC2 and TRPV1 (Fig. 5C). To further validate this finding, we carried out endogenous co-immunoprecipitation of these channels with anti-ASIC2 (ASIC2-IP) or anti-TRPV1 (TRPV1-IP) antibodies in lysates of rat aortic arch baroreceptor. The results

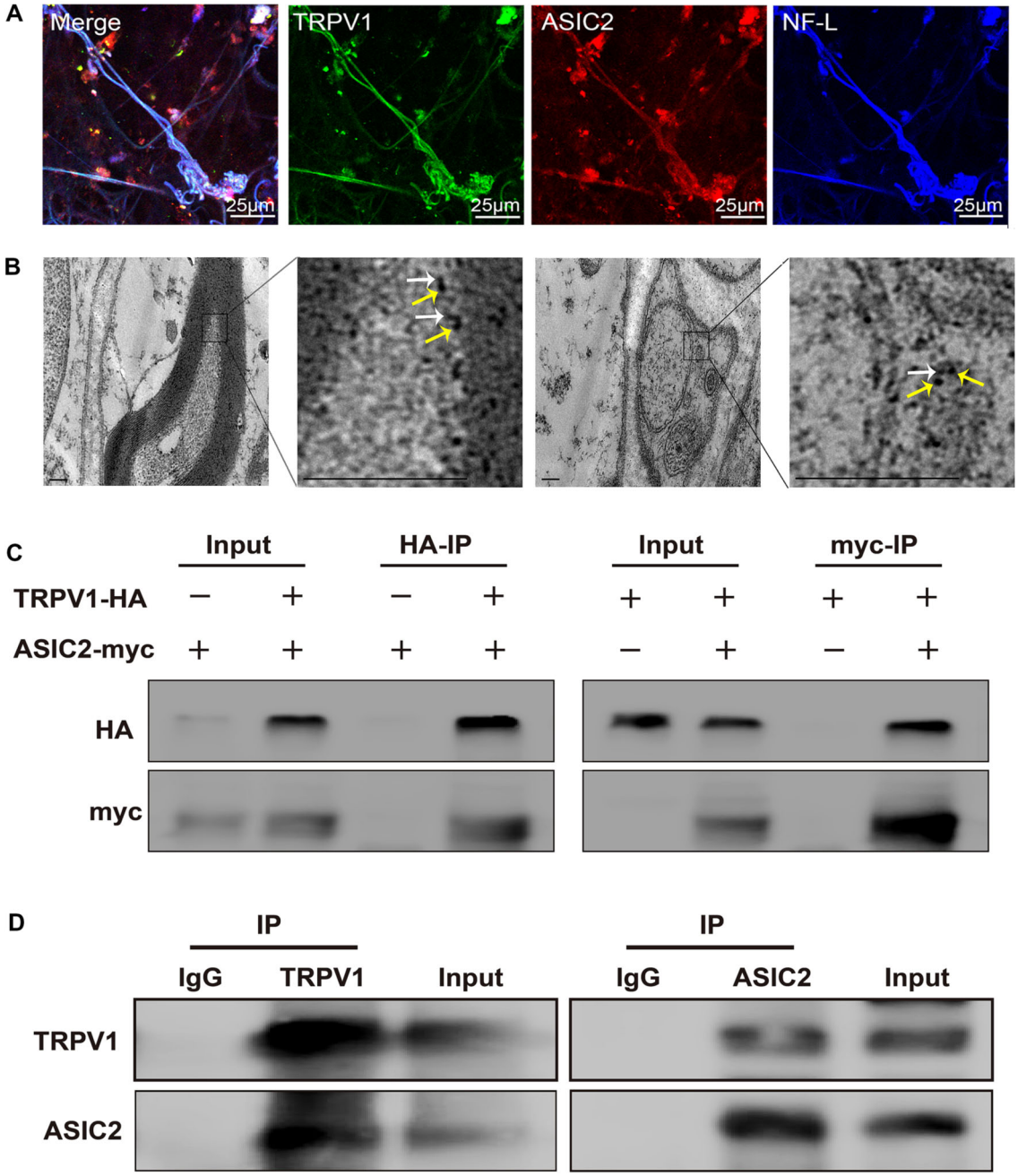

Fig. 5 ASIC2 interacts with TRPV1 by forming a compact complex in baroreceptors. **A** Representative images showing the immunoreactivity of ASIC2 (red), TRPV1 (green), and the neurofilament marker NF-L (blue) in baroreceptor terminals within the aortic arch adventitia. **B** Representative immunoelectron microscopic images of myelinated and unmyelinated nerve fibers from rat aortic baroreceptor nerve terminals. White arrows mark the 4-nm colloidal gold particles labelling ASIC2 ion channels. Yellow arrows mark 18-nm colloidal gold particles labelling TRPV1 ion channels. Scale bar, 200 nm. **C** Co-immunoprecipitation (IP) experiments carried out on lysates of HEK293T cells expressing ASIC2-myc and/or TRPV1-HA. The transfected constructs are indicated above. Anti-HA (HA-IP, left) or anti-myc (myc-IP, right) antibodies were used for IP. The antibodies used for western blotting (WB) analysis are shown on the left. **D** Co-IP experiments carried out on rat aortic arch baroreceptor tissue lysates. Left: ASIC2 and TRPV1 detected by WB analysis of immunoprecipitate collected with anti-TRPV1 antibodies (TRPV1-IP). Right: TRPV1 and ASIC2 detected by WB in immunoprecipitate collected with anti-ASIC2 antibodies (ASIC2-IP).

demonstrated that ASIC2 co-precipitated with TRPV1 and *vice versa* (Fig. 5D), indicating that endogenous ASIC2 and TRPV1 likely interact in the baroreceptors of the rat aortic arch. Immunoprecipitates from lysates treated with either anti-ASIC2 (ASIC2-IP) or anti-TRPV1 (TRPV1-IP) contained both ASIC2 and TRPV1 channel proteins as

detected by anti-ASIC2 and anti-TRPV1 western blotting (WB) analysis (Fig. 5D). Samples of the rat aortic arch baroreceptor lysate before immunoprecipitation was used as a positive control, and a mock immunoprecipitation with anti-IgG antibody was used as a negative control. Altogether, the co-distribution, the functional cooperation, and the structural interaction provide strong evidence that ASIC2 and TRPV1 form compact complexes in the baroreceptors of the rat aortic arch.

ASIC2 Interacts with TRPV1 Directly *via* Multiple Binding Sites

The previous results suggested that ASIC2 and TRPV1 form a compact complex. To investigate whether these two proteins directly interact with each other, we simulated protein-protein docking using homology models of mouse ASIC2 and TRPV1 (Fig. 6A, B). The upper and lower crown structures of the two proteins fluctuated greatly, and stable interactions did not readily occur in these regions. In contrast, stable contacts were formed on the ring section of the two proteins containing primarily hydrophobic amino-acids (Fig. S3A) and just a small proportion of hydrophilic amino-acids.

To identify the amino-acids involved in the interaction, we calculated the hydrogen bond network between ASIC2 and TRPV1 using the RINalyzer plug-in for Cytoscape 3.2 software. A large number of contacts were predicted at the protein interface. We identified all amino-acids within a 5 Å range for each protein (Fig. S3B). The homology modelling of ASIC2 and TRPV1 is shown in Fig. 6A, and the hydrogen bonds between the two proteins were divided into four distinct regions: H bonds A, H bonds B, H bonds C, and H bonds D (Fig. 6B). Specifically, the following hydrogen bonds were predicted: Glu537-Tyr70, Arg535-Phe68, Thr469-Tyr67, Val470-Tyr70, Tyr54-Ser61, Glu571-Arg42, Leu576-Arg42, Cys579-Leu44, Gln562-Val43, Gln561-Val43, Ser484-Arg41, Tyr488-Tyr453, and Asn438-Leu450. These data support the possibility of ASIC2-TRPV1 complex formation.

Both ASIC2 and TRPV1 are multi-transmembrane proteins, and the previous results showed that ASIC2 and TRPV1 likely bind directly through their extracellular domains (Fig. 6B, H bonds A, H bonds B); however, the extracellular segments of TRPV1 in H bonds A and H bonds B (Fig. 6B) are so short that it is difficult to express the protein fragments directly *in vitro*. To confirm the data predicted from the protein modeling analysis, we constructed tagged plasmids of predicted binding sites, such as, the extracellular segment of ASIC2 (ASIC2 (aa 59–427)-3×Flag) and three fragments of TRPV1: (aa 455–472)-myc-GFP, (aa 533–536)-myc-GFP, and (aa 499–511)-myc-GFP). Then, we verified the interaction sites between ASIC2 and TRPV1 by co-IP experiments (Fig. 6C). WB analysis showed that the extracellular ASIC2 segment (aa 59–427)-3×Flag combined with the extracellular TRPV1 fragments (aa 455–472)-myc-GFP and (aa 533–536)-myc-GFP (Fig. 6C) but not with the intracellular TRPV1 fragment (aa 499–511)-myc-GFP (Fig. 6C), demonstrating that binding between ASIC2 and TRPV1 is restricted to their extracellular domains. In addition, these results support the reliability of the above protein model analysis. Peptides of <30 amino-acids can also be accessed in a straightforward manner *via* solid-phase peptide synthesis, thus enabling the facile introduction of functional chemical handles and non-natural residues [29]. We then performed biotin pull-down assays using the purified recombinant GST-ASIC2 extracellular fragment (aa 59–427) and biotin-labeled mouse TRPV1 peptides (aa 455–472, aa 499–511, and aa 533–536) to verify the specificity of the interaction between ASIC2 and TRPV1 under cell-free conditions. The signal mass spectra of these peptides and the results of biotin-pulldown assays are shown in Fig. S4A, B. These results further confirmed the reliability of the above results.

Discussion

Despite the essential roles of several MSCs such as ASIC2, TRPV1, TRPC5, and PIEZO in the conversion of mechanical signals into receptor potentials in arterial baroreceptors [3, 4, 6, 7, 11, 16], the mechanism and mode of their involvement in mechano-electrical transduction remains controversial. Previous studies of MSCs have reported the performance of these channels separately; thus, whether there is cooperation between these channels has not been considered. Our results provide new evidence of synergism between MSCs in the mechano-electrical transduction of baroreceptors. Among these MSCs, ASIC2 and TRPV1 have been widely studied as molecular mediators in the conversion of mechanical signals to receptor potentials. In the present study, we found that both ASIC2 and TRPV1 are required for mechano-electrical transduction. Both the ASIC2 blocker benzamil and the TRPV1 blocker capsazepine inhibited the pressure-dependent discharge of baroreceptors in a dose-dependent manner (Figs. 1C–E and 2C–E). Moreover, when ASIC2 activity was suppressed, TRPV1 could not perform mechano-electrical transduction alone. Similarly, when TRPV1 was suppressed, ASIC2 could not perform mechano-electrical transduction, either. That is to say, after blocking either ASIC2 or TRPV1, the mechanical electrical transduction of the aortic baroreceptor does not show compensatory function. Given that both ASIC2 and TRPV1 play a critical role in the mechano-electrical transduction process of the aortic baroreceptor

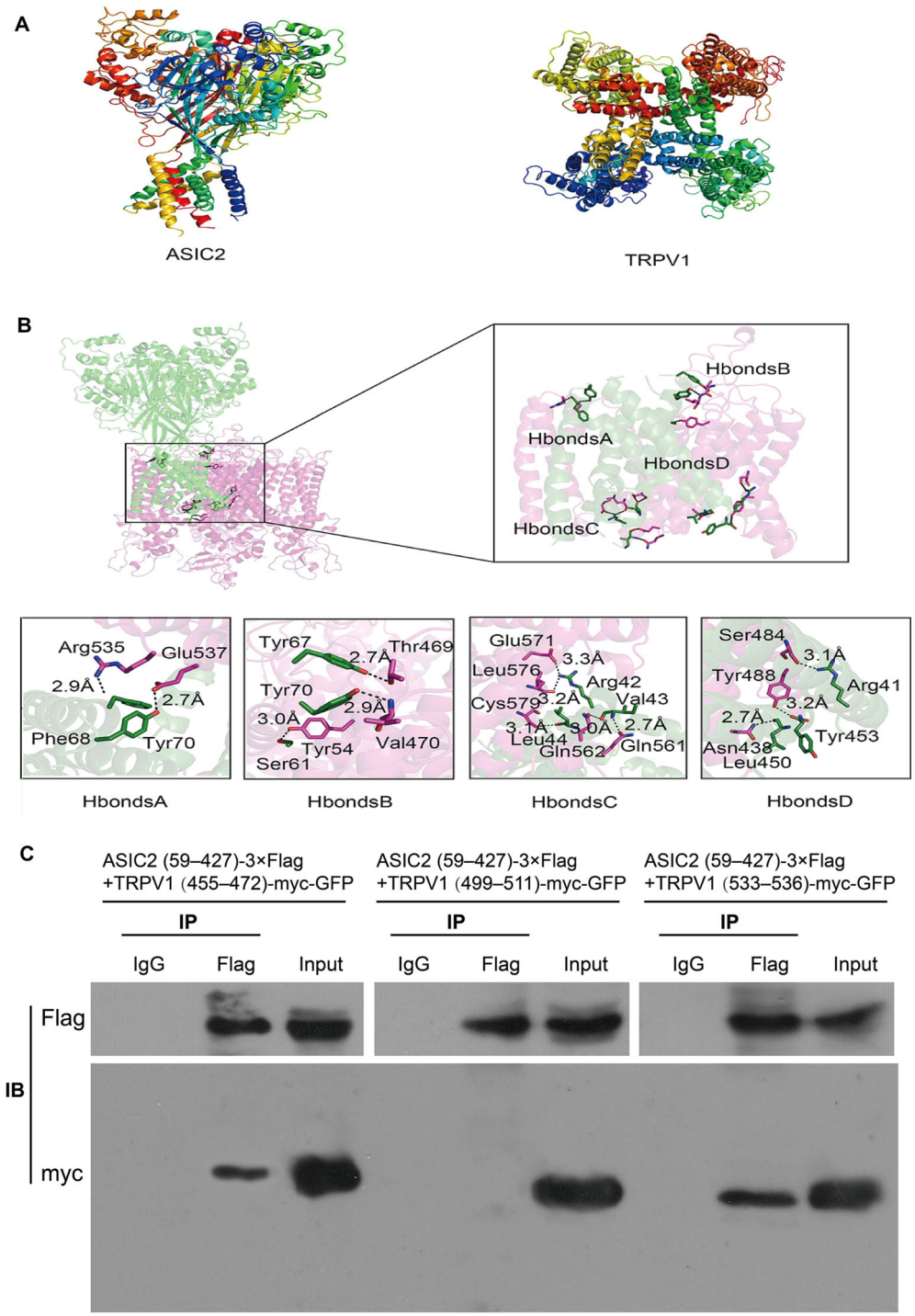

Fig. 6 ASIC2 interacts with TRPV1 directly *via* multiple binding sites. **A** Structures of ASIC2 and TRPV1 proteins. **B** Possible binding sites of ASIC2 and TRPV1, shown with 4 potential hydrogen bonds. **C** Co-immunoprecipitation (IP) experiments carried out on lysates of HEK293T cells expressing ASIC2(59–427)-3×Flag + TRPV1 (455–472)-myc-GFP, ASIC2(59–427)-3×Flag + TRPV1 (499–511)-myc-GFP, and ASIC2(59–427)-3×Flag + TRPV1(533–536)-myc-GFP. The transfected constructs are indicated above. Anti-Flag antibody was used for IP. The Flag and myc antibodies used for Western Blotting (WB) analysis are shown on the left.

[3, 4], when either of them is blocked, the other should function to compensate if there is no correlation between them, thus partly maintaining the transduction. However, we did not find this phenomenon. Therefore, we hypothesized that their functions in mechano-electrical transduction in aortic baroreceptors are co-dependent. In other

words, there is a synergy between ASIC2 and TRPV1. These results suggested that there is functional cooperation between ASIC2 and TRPV1.

To evaluate this relationship, patch-clamp experiments were carried out in HEK293T cells. WB showed that ASIC2 and TRPV1 were expressed effectively in HEK293T cells (Fig. S2A). The activity of ASIC2 markedly increased with negative pressure and returned to basal levels when the negative pressure was removed (Fig. 3A, C). Some studies have suggested that TRPV1 is insensitive to membrane stretching in heterologous over-expression systems [12]. Our results showed that the activity of TRPV1 was much weaker (Fig. 3B–D). However, compared with HEK293T cells expressing either ASIC2 or TRPV1 alone, the stretch-activated currents in cells co-expressing ASIC2 and TRPV1 were markedly increased under various negative pressure conditions (Fig. 3E). These results indicated that ASIC2 and TRPV1 function synergistically in the mechano-electrical transduction of baroreceptors.

Interestingly, inhibition of ASIC2 completely abrogated stretch-activated currents, while inhibiting TRPV1 only partially reduced these currents under negative-pressure conditions (Fig. 4). This was not fully consistent with the finding that blocking either channel completely prevented pressure-dependent discharge in arterial baroreceptors (Figs 1 and 2). Although ASIC2 was sensitive to stretch when expressed alone, the receptor potential generated by ASIC2 activation alone may not be high enough to induce action potentials or baroreceptor nerve discharge. Moreover, TRPV1 could not be activated without activation of ASIC2 when the two were co-expressed. In other words, ASIC2 and TRPV1 play a synergistic role in the mechano-electrical transduction of aortic arch baroreceptors. To our knowledge, our research is the first to demonstrate this and to show that ASIC2 and TRPV1 channels are functionally indispensable.

Identification of the DEG/ENaC/ASIC and transient receptor potential ion channel (TRP) families in baroreceptors indicated the possible existence of MSC complexes. Indeed, a large body of evidence indicates that TRP channels can be assembled into channel complexes. For example, TRPV1 co-immunoprecipitates with TRPA1 from heterologous expression systems and sensory neurons [30, 31], and this complex plays an important role in the transmission of pain. TRPV1 also interacts with members of different channel families. For example, TRPV1 interacts with large-conductance calcium-activated potassium (BK) channels by forming a TRPV1-BK complex that participates in the regulation of pain signal transduction in the peripheral nervous system [32]. To investigate the mechanisms by which ASIC2 and TRPV1 might act synergistically, we carried out immunofluorescence staining, immunoelectron microscopy, and co-IP assays. The results demonstrated that ASIC2 and TRPV1 can form a compact complex in a heterologous expression system as well as in the baroreceptors of the aortic arch (Fig. 5). To further clarify the potential interaction patterns between ASIC2 and TRPV1, we used protein modeling analysis and found that ASIC2 and TRPV1 might interact directly *via* hydrogen bonds (Figs S3 and 6A, B). To validate the data predicted from the protein modeling analysis, we used exogenous co-IP assays and biotin pull-down assays to determine whether AISC2 and TRPV1 bind directly in HEK293T cells and under cell-free conditions. In expressing HEK293T cells, there was a direct interaction between an extracellular fragment of ASIC2 (aa 59–427) and the extracellular segments of TRPV1 (aa 455–472 and aa 533–536) (Fig. 6C). The biotin pull-down assays also demonstrated the specific extracellular binding between ASIC2 and TRPV1 and thus supported the reliability of the above protein model analysis.

MSC proteins can also affect the functions of each other by regulating downstream signaling molecules. For example, TRPA1 activation causes Ca^{2+} influx, triggering Ca^{2+}-dependent phosphatases, which in turn desensitize TRPV1 activity [33]. If the distance between two channels is close enough, the local potentials (receptor potentials) produced by the channel currents can add together to trigger an action potential. This mechanism may exist in the ASIC2 and TRPV1 complex. Because blocking TRPV1, ASIC2, or PIZEO blocks the baroreceptor nerve discharges, these channels are believed to play key roles in the process of baroreceptor mechano-electrical transduction [3, 7, 11]. However, whether these channels interact or work together had not been studied. Our findings provide a new mode of MSC function in the mechanoreceptor transduction process, i.e., a synergistic mechanism between different channels.

In recent years, it has been suggested that the arterial baroreceptor reflex participates in the long-term regulation of blood pressure [34, 35], and pressure-dependent discharges from the carotid sinus nerve are significantly reduced in correlation with a decrease in TRPV1 protein expression in baroreceptors from spontaneously-hypertensive rats [36]. In addition, symptoms of high blood pressure and a marked decline in aortic nerve activity have been found in ASIC2-knockout mice [3]. This effect may largely be due to a lack of ASIC2-related functions resulting in the reduction of TRPV1 mechano-sensitivity, an increase in the threshold of the arterial baroreceptor reflex, and insensitivity to changes in blood pressure. Thus, bringing to light the physical and functional interaction between ASIC2 and TRPV1 in baroreceptors will not only help us to better understand their role in mechano-electrical transduction, but also introduces a novel mode of MSC

function in which different channels work synergistically in the mechanoreceptor transduction process. These findings also provide further clues into the role of abnormal baroreflexes in the occurrence and development of hypertension.

Further studies are still needed to uncover the molecular mechanism of the synergy between ASIC2 and TRPV1 in mechano-electrical transduction. The idea that MSCs have synergistic actions in arterial baroreceptors may also be applicable to other candidate molecules, such as ENaC, TRPC5, and PIEZO.

Conclusions

Our research provides a novel mechanism implicating both ASIC2 and TRPV1 in mechano-electrical transduction. ASIC2 is activated by stretch as a mechanosensor, while TRPV1 is more likely to be activated subsequent to ASIC2 activation and act as an amplifier of the cellular mechanosensory signaling cascades. During mechano-electrical transduction in baroreceptors, ASIC2 synergizes with TRPV1 *via* direct interaction at multiple binding sites. Our study suggests that further investigation of the potential crosstalk or synergistic actions among other MSCs is warranted.

Acknowledgements This work was supported by the National Natural Science Foundation of China (31871147 and 31371162) and the Science and Technology Development Program of Beijing Municipal Education Commission (KZ202010025038).

Conflict of interest The authors claim that there are no conflicts of interest, financial or otherwise.

References

1. Tu HY, Zhang DZ, Li YL. Cellular and molecular mechanisms underlying arterial baroreceptor remodeling in cardiovascular diseases and diabetes. Neurosci Bull 2019, 35: 98–112.
2. Cheng ZJ, Wang R, Chen QH. Autonomic regulation of the cardiovascular system: diseases, treatments, and novel approaches. Neurosci Bull 2019, 35: 1–3.
3. Lu YJ, Ma XY, Sabharwal R, Snitsarev V, Morgan D, Rahmouni K. The ion channel ASIC2 is required for baroreceptor and autonomic control of the circulation. Neuron 2009, 64: 885–897.
4. Inoue R, Jian Z, Kawarabayashi Y. Mechanosensitive TRP channels in cardiovascular pathophysiology. Pharmacol Ther 2009, 123: 371–385.
5. Drummond HA, Welsh MJ, Abboud FM. ENaC subunits are molecular components of the arterial baroreceptor complex. Ann N Y Acad Sci 2001, 940: 42–47.
6. Lau OC, Shen B, Wong CO, Tjong YW, Lo CY, Wang HC, *et al*. Author Correction: TRPC5 channels participate in pressure-sensing in aortic baroreceptors. Nat Commun 2018, 9: 16184.
7. Zeng WZ, Marshall KL, Min S, Daou I, Chapleau MW, Abboud FM, *et al*. PIEZOs mediate neuronal sensing of blood pressure and the baroreceptor reflex. Science 2018, 362: 464–467.
8. Grundy L, Caldwell A, Garcia Caraballo S, Erickson A, Schober G, Castro J, *et al*. Histamine induces peripheral and central hypersensitivity to bladder distension via the histamine H1 receptor and TRPV1. Am J Physiol Renal Physiol 2020, 318: F298–F314.
9. Kentish SJ, Frisby CL, Kritas S, Li H, Hatzinikolas G, O'Donnell TA, *et al*. TRPV1 channels and gastric vagal afferent signalling in lean and high fat diet induced obese mice. PLoS One 2015, 10: e0135892. https://doi.org/10.1371/journal.pone.0135892.
10. Wu SY, Chen WH, Hsieh CL, Lin YW. Abundant expression and functional participation of TRPV1 at Zusanli acupoint (ST36) in mice: mechanosensitive TRPV1 as an "acupuncture-responding channel." BMC Complement Altern Med 2014, 14: 96.
11. Sun H, Li DP, Chen SR, Hittelman WN, Pan HL. Sensing of blood pressure increase by transient receptor potential vanilloid 1 receptors on baroreceptors. J Pharmacol Exp Ther 2009, 331: 851–859.
12. Nikolaev YA, Cox CD, Ridone P, Rohde PR, Cordero-Morales JF, Vásquez V, *et al*. Mammalian TRP ion channels are insensitive to membrane stretch. J Cell Sci 2019, 132: jcs238360.
13. Abboud FM, Benson CJ. ASICs and cardiovascular homeostasis. Neuropharmacology 2015, 94: 87–98.
14. Page AJ, Brierley SM, Martin CM, Price MP, Symonds E, Butler R, *et al*. Different contributions of ASIC channels 1a, 2, and 3 in gastrointestinal mechanosensory function. Gut 2005, 54: 1408–1415.
15. Wu JJ, Leng TD, Jing L, Jiang N, Chen DJ, Hu YJ, *et al*. Two di-leucine motifs regulate trafficking and function of mouse ASIC2a. Mol Brain 2016, 9: 9.
16. Cabo R, Alonso P, Viña E, Vázquez G, Gago A, Feito J, *et al*. ASIC2 is present in human mechanosensory neurons of the dorsal root ganglia and in mechanoreceptors of the glabrous skin. Histochem Cell Biol 2015, 143: 267–276.
17. Wang X, Miyares RL, Ahern GP. Oleoylethanolamide excites vagal sensory neurones, induces visceral pain and reduces short-term food intake in mice via capsaicin receptor TRPV1. J Physiol 2005, 564: 541–547.
18. Alvarez de la Rosa D, Zhang P, Shao D, White F, Canessa CM. Functional implications of the localization and activity of acid-sensitive channels in rat peripheral nervous system. Proc Natl Acad Sci U S A 2002, 99: 2326–2331.
19. Xin F, Cheng Y, Ren J, Zhang ST, Liu P, Zhao HY, *et al*. The extracellular loop of the auxiliary β1-subunit is involved in the regulation of BKCa channel mechanosensitivity. Am J Physiol Cell Physiol 2018, 315: C485–C493.
20. Kaczor AA, Jörg M, Capuano B. The dopamine D2 receptor dimer and its interaction with homobivalent antagonists: homology modeling, docking and molecular dynamics. J Mol Model 2016, 22: 203.
21. Simon A, Shenton F, Hunter I, Banks RW, Bewick GS. Amiloride-sensitive channels are a major contributor to mechanotransduction in mammalian muscle spindles. J Physiol 2010, 588: 171–185.
22. Page AJ, Brierley SM, Martin CM, Hughes PA, Blackshaw LA. Acid sensing ion channels 2 and 3 are required for inhibition of visceral nociceptors by benzamil. Pain 2007, 133: 150–160.
23. Ducrocq GP, Estrada JA, Kim JS, Kaufman MP. Blocking the transient receptor potential vanilloid-1 does not reduce the exercise pressor reflex in healthy rats. Am J Physiol Regul Integr Comp Physiol 2019, 317: R576–R587.
24. Yang MH, Jung SH, Sethi G, Ahn KS. Pleiotropic pharmacological actions of capsazepine, a synthetic analogue of capsaicin,

against various cancers and inflammatory diseases. Molecules 2019, 24: E995.
25. Correll CC, Phelps PT, Anthes JC, Umland S, Greenfeder S. Cloning and pharmacological characterization of mouse TRPV1. Neurosci Lett 2004, 370: 55–60.
26. Cahusac PM. Effects of transient receptor potential (TRP) channel agonists and antagonists on slowly adapting type II mechanoreceptors in the rat sinus hair follicle. J Peripher Nerv Syst 2009, 14: 300–309.
27. Kullmann FA, Shah MA, Birder LA, de Groat WC. Functional TRP and ASIC-like channels in cultured urothelial cells from the rat. Am J Physiol Renal Physiol 2009, 296: F892–F901.
28. Jansen C, Shimoda LMN, Kawakami JK, Ang L, Bacani AJ, Baker JD, *et al*. Myrcene and terpene regulation of TRPV1. Channels (Austin) 2019, 13: 344–366.
29. Spicer CD, Jumeaux C, Gupta B, Stevens MM. Peptide and protein nanoparticle conjugates: versatile platforms for biomedical applications. Chem Soc Rev 2018, 47: 3574–3620.
30. Fischer MJ, Balasuriya D, Jeggle P, Goetze TA, McNaughton PA, Reeh PW, *et al*. Direct evidence for functional TRPV1/TRPA1 heteromers. Pflugers Arch 2014, 466: 2229–2241.
31. Staruschenko A, Jeske NA, Akopian AN. Contribution of TRPV1-TRPA1 interaction to the single channel properties of the TRPA1 channel. J Biol Chem 2010, 285: 15167–15177.
32. Wu Y, Liu YF, Hou PP, Yan ZH, Kong WJ, Liu BY, *et al*. TRPV1 channels are functionally coupled with BK(mSlo1) channels in rat dorsal root ganglion (DRG) neurons. PLoS One 2013, 8: e78203. https://doi.org/10.1371/journal.pone.0078203.
33. Akopian AN, Ruparel NB, Jeske NA, Hargreaves KM. Transient receptor potential TRPA1 channel desensitization in sensory neurons is agonist dependent and regulated by $TRPV_1$-directed internalization. J Physiol 2007, 583: 175–193.
34. Thrasher TN. Baroreceptors, baroreceptor unloading, and the long-term control of blood pressure. Am J Physiol Regul Integr Comp Physiol 2005, 288: R819–R827.
35. Thrasher TN. Arterial baroreceptor input contributes to long-term control of blood pressure. Curr Hypertens Rep 2006, 8: 249–254.
36. Yu W, Liao Y, Huang YQ, Chen SY, Sun Y, Sun CF, *et al*. Endogenous hydrogen sulfide enhances carotid sinus baroreceptor sensitivity by activating the transient receptor potential cation channel subfamily V member 1 (TRPV1) channel. J Am Heart Assoc 2017, 6: e004971.